INTERACTION STUDIES AND GAMMA-RAY PROPERTIES OF SOME LOW-*Z* MATERIALS

by

Rameshwar R. BHOSALE [1*], ***Dhammajyot K. GAIKWAD*** [1], ***Pravina P. PAWAR*** [1], ***and Madhav N. RODE*** [2]

[1]Department of Physics, Dr. Babasaheb Ambedkar Marathwada University, Aurangabad, India
[2]Department of Physics, Vaidyanath College, Parli-Vaijnath, India

Scientific paper
DOI: 10.2298/NTRP1602135B

In present work we use NaI(Tl) detector in narrow-beam good geometry set-up for the gamma ray attenuation studies of some low-*Z* materials. The parameters such as mass attenuation coefficients, effective atomic numbers and effective electron densities, atomic cross-sections, electronic cross-sections of materials for graphitic powder, polycarbonate, polyvinyl chloride, plaster of Paris, gypsum, and limestone were determined using gamma ray sources ^{57}Co, ^{133}Ba, ^{137}Bs, ^{60}Co, and ^{22}Na at energies of 122, 356, 511, 662, 840, 1170, 1275, and 1330 keV. It was observed that the effective atomic numbers and effective electron densities initially decrease and tend to be almost constant as a function of gamma-ray energy. An attempt was done to check the availability of these low-*Z* materials at large scales and obtainable at low cost as gamma ray shielding materials. The investigated data are useful in electronic industry, plastic industry, building materials, and agriculture fields.

Key words: mass attenuation coefficient, atomic cross-section, effective atomic number, low-Z material

INTRODUCTION

The investigation of mass attenuation coefficient, effective atomic number, and electron density of materials are the most important in the study of radiation in many fields. Nuclear radiation consists of high-energetic photons. The interaction of gamma rays with matter is wide spread application in nuclear physics, electronic industry, material modification, medical science, coating, paint industry, agriculture industry, *etc*. The interaction process mainly depends upon the intensity and the type of absorbing material. The gamma rays have greater penetrating power and obey different absorption laws [1]. As the use of radiation is wider for different applications, it is very important to study the interaction and absorption of gamma radiations in materials. For the study of absorption and interaction the basic quantities are effective atomic number, electron density and mass attenuation coefficient [2]. The study of attenuation coefficient gives more importance to materials in the energy range 10-1500 keV. The gamma radiation in the energy region 200 keV to 1500 keV interacts with material mainly due to a dominance of photoelectric and Compton effect photon interaction processes. Mass attenuation coefficient (μ_m) is the measure of the probability in gamma ray interaction with matter [3]. The composite materials are synthesized materials from one or more constituent materials. The composite materials are widely used in various fields such as naval, aerospace, automotive industry, and technology. This is due to their unique attributes such as non-existence of erosion, rust and high resistibility at high temperature. Owing to these advances the composite materials are popular in industrial applications [4].

Over the last 20 years of investigations infusion research all fusion devices have implemented low-*Z* carbon based materials as plasma facing materials, as they enhance the performance of these materials such as density, temperature and energy confinement [5]. The devices prepared from low-*Z* materials have the excellent thermo-mechanical properties and due to this will not melt at normal heat. The low-*Z* elements show the advanced properties when use carbon as dopants or coatings [6]. Developing new advanced materials in recent years for nuclear science has become increasingly critical to high demand on better shielding in extreme environments. Radiation shielding materials possess good mechanical properties long term reliability with suitable thermo-physical characteristics [7]. The correct values of mass attenuation coefficient are found of immense importance for various fields such as nuclear diagnosis, radiation protection, nuclear medicine, radiation dosimetry, radiation biophysics, *etc*. The mass attenuation coefficient data are

* Corresponding author; e-mail: physicsram111@gmail.com

also used in penetration and energy deposition in shielding and other dosimetric materials. In composite materials the single number cannot represent the atomic number, the number for composite materials is termed "effective atomic number (Z_{eff})" and it varies with energy. The energy absorption will be calculated if certain constants are known *i. e.*, effective atomic number (Z_{eff}) and electron density (N_{el}) of the materials, therefore the study of effective atomic number and electron density is very useful for many applications: in UV-sunlight protection, coatings, paints, electronic industry as well as medical field [8]. Recently few researchers in our laboratory investigated the values of mass attenuation coefficient, effective atomic numbers, electron densities, total atomic cross-section for dosimetric materials, fatty acid, minerals, amino acids, low-Z materials, *etc*.[9-12]. Many researchers investigated the extensive data on effective electron density, electron density, atomic cross-section, total cross-section for many materials [13-15].

The objective of the experimental work is to investigate gamma ray attenuation in these samples as low-Z materials are affordable as compared to high-Z materials such as lead, mercury which may not prove useful at large dimensions. Gamma ray attenuation study is very useful to check the feasibility of the materials. We have measured the mass attenuation coefficient (μ_m) which was then used to calculate total attenuation cross-section (σ_t). The attenuation data for theoretical calculations is obtained from XCOM program using a PC [16, 17]. It shows good agreement with the experimental data for some low-Z materials.

THEORY

In present work the following equations were used to determine the mass attenuation coefficient, atomic cross-sections (σ_t), electronic cross-sections (σ_e), effective atomic numbers (Z_{eff}) and effective electron densities (N_{eff}) and molar extinction coefficient for low-Z materials.

When a beam of monochromatic gamma photons is attenuated on matter according to Lambert-Beer law:

$$I = I_0 e^{-\mu t} \tag{1}$$

where, I_0 and I are the incident and transmitted photon intensities, respectively, μ [cm^{-1}] represents linear attenuation coefficient of the material and t [cm] is the thickness of the target material/sample. Rearrangement of eq. (1) yields the following equation for the linear attenuation coefficient

$$\mu = \frac{1}{t} \ln \frac{I_0}{I} \tag{2}$$

The mass attenuation coefficients μ_m of the sample should be calculated by using the equation

$$\mu_m = \sum_i w_i (\mu_m)_i \tag{3}$$

where w_i is the weight fraction. The w_i can be defined as follows

$$w_i = \frac{n_i A_i}{\sum_i n_i A_i} \tag{4}$$

where A_i is the atomic weight of the sample and n_i the number of formula units.

The values of mass attenuation coefficients, eq. (3), were then used to determine the total attenuation cross-section (σ_{tot}) by the following relation

$$\sigma_{tot} = \mu_m \frac{N}{N_A} \tag{5}$$

where $N = \sum_i n_i A_i$ is the atomic mass of the sample and N_A is the Avogadro's number.

Similarly, effective electronic cross-section (σ_e) for the individual element is given by

$$\sigma_e = \frac{1}{N_A} \sum_i \frac{f_i A_i}{Z_i} (\mu_m)_i = \frac{\sigma_{t,a}}{Z_{eff}} \tag{6}$$

where f_i is the fractional abundance of the sample and Z_i – the atomic number of the sample.

The total atomic cross-section and total electronic cross-section are related with the effective atomic number. Therefore the equation for Z_{eff} can be defined as

$$Z_{eff} = \frac{\sigma_t}{\sigma_e} \tag{7}$$

The equation for N_{eff} can be defined as

$$N_{eff} = \frac{N_A}{N} Z_{eff} \tag{8}$$

EXPERIMENTAL DETAILS

Radioactive sources ^{57}CO, ^{133}Ba, ^{137}Cs, ^{54}Mn, ^{60}CO, and ^{22}Na emitting energies 122, 356, 511, 662, 840, 1170, 1275, and 1330 keV, respectively, were used for irradiation. The gamma ray photons were detected using NaI(Tl) detector with resolution of 0.101785 to 662 keV. A detailed experimental set-up of transmission experimental is shown in fig. 1. Signals from the detector were enlarged and analyzed with 8K multichannel analyzer. The effectiveness of NaI(Tl) detector is higher at low source energy [18]. The uncertainty in determined experiment is found to be 1-4 % [19]. To make graphitic powder (c), polycarbonate ($C_{15}H_{16}O_2$), polyvinyl chloride (C_2H_3Cl), plaster of Paris ($Ca_2S_2O_9H$), gypsum ($CaSO_4H_4O_2$), and limestone ($CaCO_3$) as radiation target we used KBr press machine to prepare tablets having same thickness (0.13 g/cm^2). Then we filled them in a cylindrical plastic container having the same diameter as that of sample tablets. To determine the diameters of these samples we used a traveling microscope. Transmission experiment was performed with the empty sample container and it was found that the

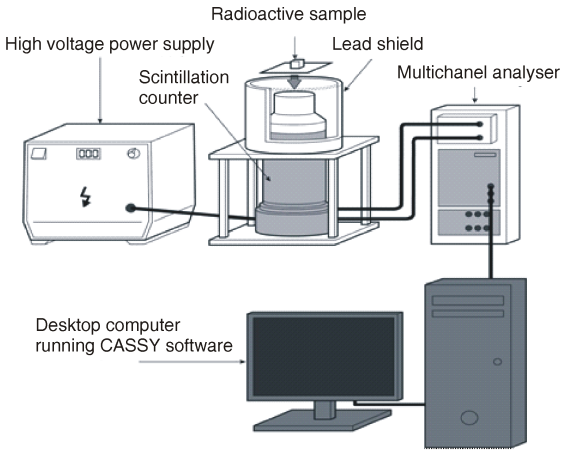

Figure 1. Schematic diagram of experimental set-up

attenuation of photons of the empty containers was negligible.

To get accuracy in experiment we prepared tablets weighted using sensitive digital balance having accuracy 0.001 mg for each sample. Samples were weighed several times and the mean of these samples weight was taken as mass of the sample. To satisfy the ideal condition the sample thickness was selected in the order $2 < \ln(I_0/I) < 4$ [20]. Mass attenuation coefficients (μ/ρ) for all the samples of low-*Z* materials were calculated using eq. (3). The values of mass attenuation coefficients were also obtained using the XCOM program at all photon energies of current interest [17].

To optimize minor errors we took care of some conditions that are counting statistics, impurities added in the sample: The error due to the sample impurities can be high only when large percentage of high *Z* impurities is present in the sample-uniformity of the sample. The non-uniformity of the sample material introduces a fraction of error of about half the root mean square deviation in mass per unit area, dead time, proper adjustment of the distance between the detector and source ($30 \text{ cm} < d < 50 \text{ cm}$), the maximum angle of scattering was below 30 min of the NaI(Tl) detector. The photon built-up effect was kept minimum by choosing optimum count rate and the counting. Optimum transmission ratio (in the range 0.1 to 0.5) is obtained using proper selection of samples thickness in order to minimize photon build-up in the absorber. The photon built-up depends on the atomic number and the sample thickness, and also on the incident photon energy. It is also a consequence of the multiple scattering inside the sample. In the multichannel analyzer used in the present study, there was a built-in provision for dead time correction. The pulse piles of effects were kept minimum by selecting an optimum count rate and counting time.

RESULTS AND DISCUSSION

The values of mean atomic number calculated from chemical formula for graphitic powder, polycarbonate, polyvinyl chloride, plaster of Paris, gypsum, and limestone are described in tab. 1. It shows that the mean atomic number for all low-*Z* materials is different. The values of μ_m [cm^2g^{-1}] for these low-*Z* materials at energies 122, 356, 511, 662, 840, 1170, 1275, and 1330 keV calculated experimentally using NaI(Tl) detector and theoretically using XCOM are mentioned in tab. 2 and a typical plot displayed in fig. 2. Based on these values it can be seen that there is a small amount of variation in experimentally and theoretically calculated values *i. e*., it shows good agreement. The values for atomic cross-section (σ_t) are displayed in tab. 3 and a typical plot is displayed in fig. 3.

Table 1. The mean atomic numbers calculated from the chemical formula for low-*Z* materials

Low-*Z* materials	Molar mass [gmol^{-1}]	Chemical formula	Mean atomic number, <*Z*
Graphitic powder	12.01	C	6
Polycarbonate	254.3	$C_{15}H_{16}O_2$	3.6970
Polyvinyl chloride	62.50	CH = CHCl	5.333
Plaster of Parris	77.94	$Ca_2S_2O_8H_{10}$	10.35
Gypsum	136.14	$CaSO_4\ 2H_2O$	7.333
Limestone	100.08	$CaCO_3$	10.00

Table 2. Mass attenuation coefficient, μ_m [cm^2g^{-1}] of low-*Z* materials

Low-*Z* materials	Energy [keV]															
	122		356		511		662		840		1170		1275		1330	
	Exp.	Theor.	Exp.	Theor.	Exp.	Theor.	Exp.	Theor.	Exp.	Theor.	Exp.	Theor.	Exp.	Theor.	Exp.	Theor.
Graphitic powder	0.142	0.143	0.101	0.100	0.083	0.085	0.075	0.077	0.068	0.069	0.057	0.058	0.055	0.056	0.050	0.050
Polycarbonate	0.152	0.153	0.105	0.107	0.091	0.092	0.082	0.083	0.073	0.073	0.062	0.063	0.060	0.060	0.056	0.058
Polyvinyl chloride	0.160	0.162	0.114	0.115	0.097	0.097	0.086	0.088	0.077	0.078	0.066	0.067	0.058	0.059	0.061	0.062
Plaster of Paris	0.170	0.171	0.102	0.102	0.084	0.086	0.077	0.078	0.067	0.069	0.061	0.060	0.056	0.057	0.055	0.055
Gypsum	0.17	0.18	0.104	0.104	0.086	0.087	0.079	0.080	0.070	0.070	0.062	0.061	0.057	0.058	0.055	0.056
Limestone	0.280	0.282	0.105	0.107	0.081	0.082	0.073	0.074	0.065	0.065	0.056	0.058	0.052	0.053	0.053	0.053

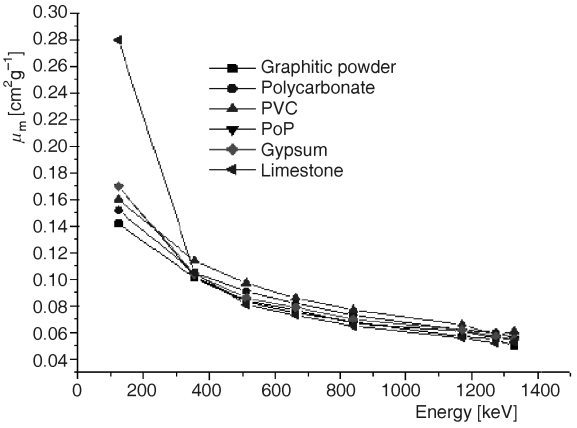

Figure 2. Typical plot of μ_m *vs.* energy for some low-*Z* materials

It can be clearly seen from fig. 3 that there is a certain variation in atomic cross-section, but as the photon energy increases the values for atomic cross-section (σ_t) decreases and at a point they are constant.

The experimental and theoretical values calculated from XCOM for electronic cross-section (σ_e) of low-*Z* materials are displayed in tab. 4. They show good agreement with the experimental and theoretical values. Figure 4 shows that only the low-*Z* material *i. e.*, polycarbonate which is having the highest mass number shows more electronic cross-sections as compared to other low-*Z* materials at the same photon energy and remains constant at a certain point. The values for effective atomic number (Z_{eff}) are displayed in tab. 5 and a typical plot in fig. 5. It can be clearly seen both from the table and figure that the plaster of Paris and limestone which are having the mean atomic number near to 10 displays more effective atomic number

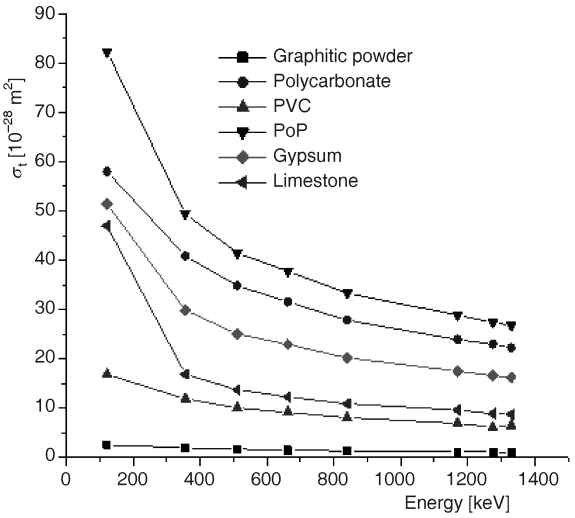

Figure 3. Typical plot of σ_t per atom *vs.* energy for some low-*Z* materials

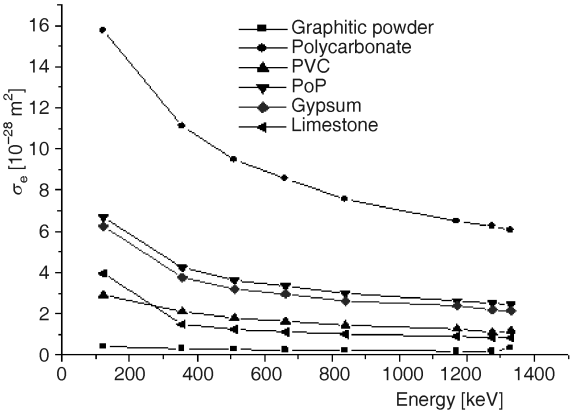

Figure 4. Typical plot of σ_e per atom *vs.* energy for some low-*Z*

Table 3. Atomic cross-sections, σ_t (10^{-28} m^2 per molecule) of some low-*Z* materials

Low-*Z* materials	Energy [keV]															
	122		356		511		662		840		1170		1275		1330	
	Exp.	Theor.	Exp.	Theor.	Exp.	Theor.	Exp.	Theor.	Exp.	Theor.	Exp.	Theor.	Exp.	Theor.	Exp.	Theor.
Graphitic powder	2.855	2.856	2.005	2.010	1.711	1.713	1.544	1.549	1.381	1.382	1.170	1.172	1.130	1.133	1.095	1.097
Polycarbonate	57.990	57.993	40.895	40.898	34.869	34.871	31.531	31.536	27.855	27.859	23.911	23.917	23.030	23.045	22.320	22.325
Polyvinyl chloride	16.850	16.852	11.951	11.954	10.070	10.076	9.210	9.214	8.089	8.094	6.980	6.983	6.121	6.122	6.521	6.527
Plaster of Paris	82.300	82.304	49.420	49.425	41.490	41.499	37.800	37.806	33.341	33.348	28.882	28.886	27.431	27.436	26.825	26.830
Gypsum	51.440	51.441	29.860	29.864	28.085	25.089	22.920	22.922	20.224	20.227	17.518	17.521	16.638	16.641	16.270	16.275
Limestone	46.982	46.984	16.895	16.897	13.753	13.756	12.309	12.311	10.910	10.915	9.665	9.669	8.874	8.876	8.803	8.805

Table 4. Electronic cross-sections, σ_e (10^{-28} m^2 per molecule) of some low-Z materials

Low-*Z* materials	Energy [keV]															
	122		356		511		662		840		1170		1275		1330	
	Exp.	Theor.	Exp.	Theor.	Exp.	Theor.	Exp.	Theor.	Exp.	Theor.	Exp.	Theor.	Exp.	Theor.	Exp.	Theor.
Graphitic powder	0.420	0.422	0.301	0.305	0.260	0.262	0.236	0.239	0.212	0.214	0.182	0.183	0.175	0.177	0.324	0.326
Polycarbonate	15.750	15.754	11.109	11.111	9.471	9.474	8.561	8.566	7.562	7.566	6.490	6.493	6.253	6.256	6.055	6.061
Polyvinyl chloride	2.917	2.920	2.111	2.113	1.790	1.793	1.642	1.647	1.451	1.453	1.259	1.261	1.104	1.107	1.179	1.182
Plaster of Paris	6.694	6.696	4.243	4.247	3.630	3.632	3.350	3.352	2.990	2.993	2.633	2.636	2.512	2.515	2.462	2.465
Gypsum	6.255	6.260	3.765	3.768	3.202	3.204	2.950	2.953	2.626	2.627	2.395	2.300	2.189	2.191	2.142	2.146
Limestone	3.956	3.960	1.498	1.501	1.243	1.244	1.124	1.128	1.007	1.011	0.905	0.911	0.837	0.840	0.8348	0.8350

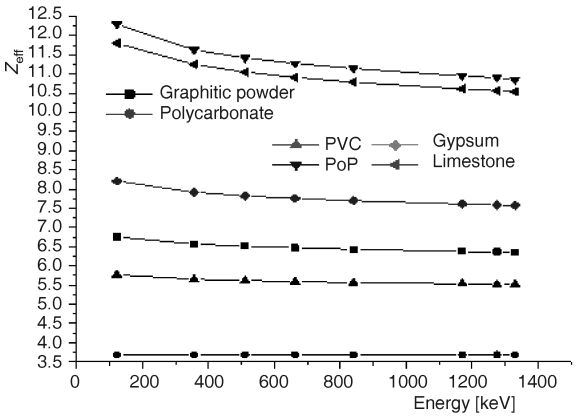

Figure 5. Typical plot of Z_{eff} *vs.* energy for some low-*Z* material

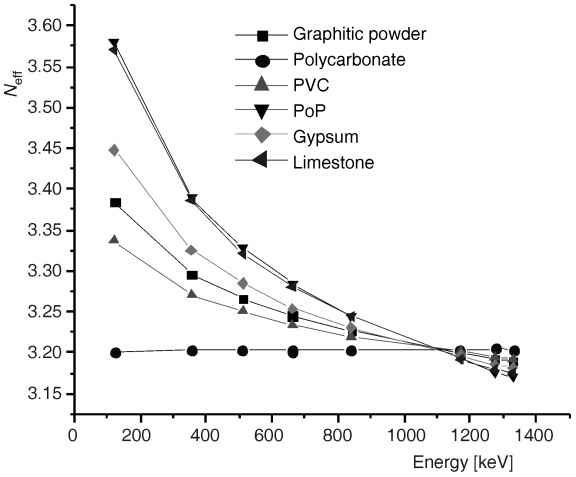

Figure 6. Typical plot of N_{eff} *vs.* energy for some low-*Z* materials

at the same energy used for the all low-*Z* materials, and remains constant at the energy point.

The effective electron density (N_{eff}) for low-*Z* materials is displayed in tab. 6 and shows good agreement with the experimental and theoretical values. Figure 6 shows that the plaster of Paris and limestone shows more effective electron density as compared to the other low-*Z* materials; it decreases slightly and remains the same at the energy point. It is clear that Z_{eff} and N_{eff} are related to each-other as values which initially decrease and then remain constant as photon energy increases.

CONCLUSIONS

The present experimental study has been undertaken to get information on mass attenuation coefficient (μ_m) and related values of (Z_{eff}, N_{eff}, σ_e and σ_t) for six low-*Z* materials. It is found that μ_m is the main physical quantity to determine the values of N_{eff} and Z_{eff} for low-*Z* materials. It can be concluded from the present work that the low-*Z* materials used in this investigation are of use in dosimetry, radiation protection, *etc*. Present investigation should be useful in medical application as low-*Z* materials are composed of C, H, N, and O constituent elements. Also, low-*Z* materials doped with the high *Z* elements can be used as radiation shielding materials and are available at low cost. The values introduced in the present investigation can be used in many applications as electronics industry, construction, plastic industry, agriculture industry, *etc*. as a gamma ray shielding materials.

Table 5. Effective atomic number, Z_{eff} of some low-*Z* materials

Low-*Z* materials	Energy [keV]															
	122		356		511		662		840		1170		1275		1330	
	Exp.	Theor.	Exp.	Theor.	Exp.	Theor.	Exp.	Theor.	Exp.	Theor.	Exp.	Theor.	Exp.	Theor.	Exp.	Theor.
Graphitic powder	6.751	6.753	6.570	6.575	6.514	6.516	6.472	6.474	6.434	6.435	6.381	6.381	6.364	6.368	6.360	6.361
Polycarbonate	3.675	3.677	3.679	3.680	3.680	3.680	3.680	3.681	3.680	3.682	3.681	3.683	3.685	3.683	3.682	3.683
Polyvinyl chloride	5.770	5.771	5.652	5.656	5.620	5.619	5.590	5.592	5.565	5.568	5.532	5.535	5.523	5.525	5.520	5.521
Plaster of Paris	12.292	12.290	11.631	11.636	11.421	11.425	11.275	11.276	11.145	11.142	10.950	10.957	10.905	10.908	10.850	10.884
Gypsum	8.211	8.216	7.920	7.923	7.825	7.829	7.758	7.761	7.699	7.70	7.611	7.615	7.590	7.592	7.580	7.581
Limestone	11.801	11.864	11.250	11.251	11.051	11.053	10.911	10.914	10.785	10.787	10.611	10.613	10.566	10.567	10.544	10.545

Table 6. Effective electron densities, N_{eff} (10^{23}) for low-*Z* materials

Low-*Z* materials	Energy [keV]															
	122		356		511		662		840		1170		1275		1330	
	Exp.	Theor.	Exp.	Theor.	Exp.	Theor.	Exp.	Theor.	Exp.	Theor.	Exp.	Theor.	Exp.	Theor.	Exp.	Theor.
Graphitic powder	3.385	3.386	3.296	3.297	3.266	3.267	3.245	3.246	3.227	3.228	3.199	3.199	3.192	3.193	3.190	3.192
Polycarbonate	3.200	3.201	3.203	3.204	3.204	3.203	3.202	3.204	3.204	3.205	3.203	3.205	3.205	3.206	3.204	3.206
Polyvinyl chloride	3.337	3.338	3.271	3.272	3.251	3.250	3.234	3.235	3.220	3.221	3.202	3.201	3.194	3.196	3.192	3.194
Plaster of Paris	3.581	3.582	3.390	3.391	3.329	3.330	3.284	3.286	3.245	3.247	3.193	3.194	3.176	3.179	3.170	3.172
Gypsum	3.448	3.450	3.325	3.327	3.285	3.288	3.254	3.259	3.231	3.232	3.197	3.198	3.185	3.188	3.182	3.183
Limestone	3.570	3.571	3.386	3.386	3.321	3.320	3.281	3.284	3.245	3.246	3.192	3.194	3.179	3.180	3.176	3.177

AUTHORS' CONTRIBUTIONS

Theoretical and experimental work was carried out by R. R. Bhosale and D. K. Gaikwad. Experimental data was analyzed by P. P. Pawar and M. N. Rode. Whole manuscript was reviewed by all authors.

REFERENCES

[1] Lilley, J., Nuclear Physics Principles and Applications 1st ed., John Willey & Sons, N. Y., USA, 2001
[2] Allah, N., Sarhan, S. S., Factors Affecting Gamma Ray Transmission, *Jordon Journal of Physics, 5* (2012), 2, pp. 78-88
[3] Kore, P. S., Pawar, P. P., Measurements of Mass Attenuation Coefficient, Effective Atomic Number and Electron Densities of Some Amino Acids, *Radn. Physand Chem., 98* (2014), May, pp. 86-91
[4] Athanassiadis, K. N., Radioactivity Control of Composite Materials Using Low Energy Photon Radiation, Chapter 14 in Advances in Composite Materials – Ecodesign and Analysis (Ed. B. Attaf,), InTech, March 2011, DOI: 103.5772/14002
[5] Philipps, V., *et al*., Comparison of Tokamak Behavior with Tungsten and Low-*Z* Plasma Facing Materials, *Plasma Phys. Control. Fusion, 42* (2000), 12B, pp. 293-310
[6] Davis, J. W., Haasz, A. A., Impurity Release from Low-*Z* Materials under Light Particles Bombardment, *Journal of Nuclear Materials, 241-243* (1997), Feb., pp. 37-51
[7] Chen, S., *et al*., Novel Light-Weight Materials for Shielding Gamma Ray, *Radn. Phys. Chem., 96* (2014), pp. 27-37
[8] Manohara, S. R., Hanagodimath, S. M., Studies on Effective Atomic Numbers and Electron Densities of Essential Amino Acids in the Energy Range1keV-100 GeV, *Nucl. Instrum. Methods Phys. Res. B, 258* (2007), 2, pp. 321-328
[9] Pawar, P. P., Bichile, G. K., Studies on Mass Attenuation Coefficient, Effective Atomic Number and Electron Density of Some Amino Acids in the Energy Range 0.122-1.330 MeV, *Radiat. Phys. Chem., 92* (2013), Nov., pp. 22-27
[10] Ladhaf, B. M., Pawar, P. P., Studies on Mass-Energy Absorption Coefficients and Effective Atomic Energy-Absorption Cross Sections for Carbohydrates, *Radiation. Phys. Chem., 109* (2014), pp. 89-94
[11] Gaikwad, D. K., *et al*., Attenuation Cross Sections Measurements of Some Fatty Acids in the Energy Range 122-1330 keV, Accepted in Pramana – Journal of Physics, 2015
[12] Kore, P. S., *et al*., Evaluation of Radiological Data of Some Saturated Fatty Acids Using Gamma Ray Spectrometry, *Radiation Physics and Chemistry, 119* (2016), Feb., pp. 74-79
[13] Singh, N., *et al*., Comparative Study of Lead Borate and Bismuth Lead Borate Glass Systems as Gamma Radiation Shielding Materials, *Nucl. Instr. Meth B., 225* (2004), 3, pp. 305-309
[14] Singh, S., *et al*., Measurements of Linear Attenuation Coefficients of Irregular Shaped Samples by Two Media Method, *Nucl. Instr. Meth., B 266* (2008), 7, pp. 1116-1121
[15] Gerward, L., *et al*., X-Ray Absorption in Matter, Reengineering Xcom, *Radiat. Phys. Chem., 60* (2001), 1-2, pp. 23-24
[16] Hubbell, J. H., Review of Photon Interaction Cross Section Data in the Medical and Biological Context, *Phys. Med. Biol., 44* (1999), 1, R1-R22
[17] Berger, M. J., Hubbell, J. H., XCOM: Photon Cross Sections Database, web version1.2, 1999. Available from: <http://physics.nist.gov/xcom>, originally published as NBSIR 87-3597:XCOM: Photon Cross Sections on a Personal Computer, Washington DC, USA
[18] Abd-Elzaher, M., *et al*., Determination of Full Energy Peak Efficiency of NaI (Tl) Detector Depending on Efficiency Transfer Principle for Conversion form Experimental Values, *World Journal of Nuclear Science and Technology, 2* (2012), 3, pp. 65-72
[19] Kacal, M. R., Han, I., Akman, F., Measurement of Mass Attenuation Coefficients by Si(Li), NaI(Tl), and Cd(Tl) Detectors, in *Nuclear Science and Technology.* 2012, pp. 59-69, ISBN: 978-81-7895-546-9
[20] Creagh, D. C., The Resolution of Discrepancies in Tables of Photon Attenuation Coefficients, *Nucl. Instrum. Methods, A 255* (1987), pp. 1-16

Received on January 9, 2016
Accepted on April 4, 2016

Рамешвар Р. БОСАЛЕ, Дамајот К. ГАИКВАД, Правина П. ПАВАР, Матхав Н. РОДЕ

ПРОУЧАВАЊЕ ИНТЕРАКЦИЈА И ОСОБИНА ГАМА ЗРАЧЕЊА МАТЕРИЈАЛА СА НИСКИМ АТОМСКИМ БРОЈЕМ Z

У истраживању коришћен је NaI(Tl) детектор и поставка геометрије уског снопа за проучавање особина слабљења гама зрачења материјала са ниским атомским бројем Z. За испитиване материјале, који су обухватали графитни прашак, поликарбонат, поливинил хлорид, гипс из Париза, гипс и кречњак, одређени су следећи параметри: масени коефицијент слабљења, ефективни атомски број, ефективна густина електрона, атомски ефикасни пресек и електронски ефикасни пресек. Као извори гама зрачења коришћени су ^{57}Co, ^{133}Ba, ^{137}Bs, ^{60}Co и ^{22}Na, на енергијама 122, 356, 511, 662, 840, 1170, 1275 и 1330 keV. Уочено је да ефективни атомски бројеви и ефективне густине електрона најпре опадају, а потом теже да задрже скоро константну вредност у зависности од енергије гама зрачења. Проверена је доступност ових материјала у великим количинама, као материјала ниских цена за заштиту од гама зрачења. Добијени подаци могу се употребити у електронској индустрији, индустрији пластике, производњи грађевинских материјала и у пољопривреди.

Кључне речи: масени коефицијент слабљења, атомски ефикасни пресек, ефективни атомски број, материјал са ниским атомским бројем Z